

Investigation of earthquake angle effect on the seismic performance of steel bridges

Ahmet C. Altunışık and Ebru Kalkan *

Department of Civil Engineering, Karadeniz Technical University, Trabzon, Turkey

(Received June 30, 2016, Revised November 01, 2016, Accepted November 02, 2016)

Abstract. In this paper, it is aimed to evaluate the earthquake angle influence on the seismic performance of steel highway bridges. Upper-deck steel highway bridge, which has arch type load bearing system with a total length of 216 m, has been selected as an application and analyzed using finite element methods. The bridge is subjected to 1992 Erzincan earthquake ground motion components in nineteen directions whose values range between 0 to 90 degrees, with an increment of 5 degrees. The seismic weight is calculated using full dead load plus 30% of live load. The variation of maximum displacements in each directions and internal forces such as axial forces, shear forces and bending moments for bridge arch and deck are attained to determine the earthquake angle influence on the seismic performance. The results show that angle of seismic input motion considerably influences the response of the bridge. It is seen that maximum arch displacements are obtained at X, Y and Z direction for 0°, 65° and 5°, respectively. The results are changed considerably with the different earthquake angle. The maximum differences are calculated as 57.06%, 114.4% and 55.71% for X, Y and Z directions, respectively. The maximum axial forces, shear forces and bending moments are obtained for bridge arch at 90°, 5° and 0°, respectively. The maximum differences are calculated as 49.12%, 37.37% and 51.50%, respectively. The maximum shear forces and bending moments are obtained for bridge deck at 0°. The maximum differences are calculated as 49.67%, and 49.15%, respectively. It is seen from the study that the variation of earthquake angle effect the structural performance of highway bridges considerably. But, there is not any specific earthquake angle of incidence for each structures or members which increases the value of internal forces of all structural members together. Each member gets its maximum value of in a specific angle of incidence.

Keywords: earthquake angle effect; finite element method; seismic performance; steel bridge

1. Introduction

Bridges can be damaged by dynamic loads such as wind, tsunami, earthquake and etc. It is known that, in case of destruction, there will be significant life and financial loses. To prevent these dramatical events after earthquakes, the structural should be carried out by expert engineers using linear and non-linear finite element analyses considering different earthquake angles. But, during the earthquakes, the implementation of motions on axial direction of each building is not possible.

Earthquake ground motions have three components with different intensity including two

*Corresponding author, Professor, E-mail: ahmetcan8284@hotmail.com

orthogonal (longitudinal and transverse) in lateral and vertical direction and in general, all design codes such as TERDC (2007), Eurocode (2004) and FEMA (2000) suggested that two lateral earthquake components should be perpendicular to each other. When take into account the effect of earthquake angle on bridge, the importance of this issue has revealed many scientific studies along.

In the literature, many papers exist about the earthquake angle influence on the structural behavior of bridges. Gonzales (1992) presented detail investigation about the earthquake direction effect on the seismic analysis. Gao *et al.* (2004) studied on multi-component seismic analysis for irregular structures. Cronin (2007) determined the response sensitivity of highway bridges to random multi-component earthquake excitation. Song *et al.* (2008) presented the study on critical angle to the seismic response of curved bridges based on pushover method. Torbol and Shinozuka (2012) developed the fragility curves of bridges using the effect of seismic incidence angle. Atak *et al.* (2014) displayed the directional effect of strong ground motion on the seismic behaviour of skewed bridges. Bortoli *et al.* (2014) exhibited the significance of ground motion incidence angle in seismic design of bridges. Understanding directionality concepts in seismic analysis emerged by Newton (2014). Ni *et al.* (2015) performed the input angle influence on seismic response of curved girder bridge. In plan, for curved bridge, including single and double directional, the impact of the earthquake has been created from 0 to 180 degrees by increasing the degrees three for each one. Also, many studies can be found in the literature about the importance of this issue on the structural response of different type of engineering structures using analytical and numerical calculations (Lopez and Torres 1997, Armouti 2002, Hernandez and Lopez 2002, Athanatopoulou 2005, Ateş *et al.* 2009, Sevim 2013, Fukumoto and Takewaki 2015, Kostinakis and Athanatopoulou 2015).

In this paper, it is aimed to determinate the earthquake angle effect on the structural behavior of arch type steel highway bridge. The nineteen different earthquake directions, whose values range between 0 to 90 degrees, with an increment of 5 degrees are taken into account for comparison. The variation of the maximum displacements and internal forces are considered to determine the influence on seismic performance.

2. Ground motion incidence angle

In order to evaluate the ground motion rotation influence, the two orthogonal (longitudinal and transverse) components of acceleration $\ddot{u}_{xg}(t)$ and $\ddot{u}_{yg}(t)$ are rotated by regarded degree and resolved to the structural degrees of freedom (Fig. 1(a)). It is affirmed that $\ddot{u}_{xg}(t)$ and $\ddot{u}_{yg}(t)$ are initially directed along to the X (longitudinal) and Y (transverse) directions, respectively. The rotation (θ) of ground motion components at counter clockwise can be resolved to equivalent ground motion components along the axes ($\ddot{u}_1(t)$ and $\ddot{u}_2(t)$) of the structural degrees of freedom.

The transformation matrix (T) is used to perform this operation and is based solely on geometry (Cronin 2007). It should be note that the term of $\ddot{u}_{zg}(t)$ shown the vertical motion which is not affected by planar rotation.

A similar approach were used in the literature (Mohraz and Tiv 1994, Liang and Lee 2003) in order to study ground motion incidence angle is to rotate the structure and transform the original ground motion components to the rotated structural degrees of freedom (Fig. 1(b)) (Cronin 2007).

$$\ddot{u}_s = T \cdot \ddot{u}_g \quad (1)$$

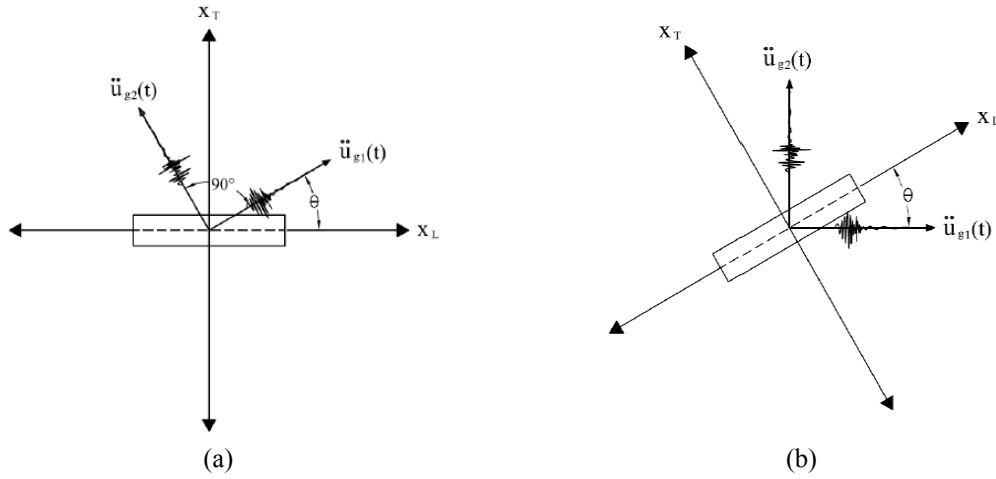


Fig. 1 Rotation of: (a) ground motion acceleration; and (b) structure

$$\begin{bmatrix} \ddot{u}_{s1}(t) \\ \ddot{u}_{s2}(t) \\ \ddot{u}_{s3}(t) \end{bmatrix} = \begin{bmatrix} \cos \theta & -\sin \theta & 0 \\ \sin \theta & \cos \theta & 0 \\ 0 & 0 & 1 \end{bmatrix} \begin{bmatrix} \ddot{u}_{xg}(t) \\ \ddot{u}_{yg}(t) \\ \ddot{u}_{zg}(t) \end{bmatrix} \tag{2}$$

$$\ddot{u}_s = T_t \cdot \ddot{u}_g \tag{3}$$

$$\begin{bmatrix} \ddot{u}_{s1}(t) \\ \ddot{u}_{s2}(t) \\ \ddot{u}_{s3}(t) \end{bmatrix} = \begin{bmatrix} \cos \theta & -\sin \theta & 0 \\ -\sin \theta & \cos \theta & 0 \\ 0 & 0 & 1 \end{bmatrix} \begin{bmatrix} \ddot{u}_{xg}(t) \\ \ddot{u}_{yg}(t) \\ \ddot{u}_{zg}(t) \end{bmatrix} \tag{4}$$

The transformation matrix T_t is basically the inverse of T and could also be thought of as the clockwise rotation of ground motion in terms of a stationary structure (Cronin 2007).

3. Description of bridge

Eynel Arch Type Steel Highway Bridge connecting to the villages near to sides of Suat Uğurlu Dam reservoir in city of Samsun, Turkey and which has also a main arch span of 186 m is selected as numerical example. This bridge was originally designed and constructed by Prokon Engineering and Consultancy, Inc. (Prokon 2007). The construction of bridge was started in 2007 and opened to traffic in 2009. Fig. 2 shows some views of the bridge.

The bridge, which consists of the steel arch ribs, vertical and lateral load bearing systems, columns, and the deck system in its structural system, is upper-deck steel bridge which has arch type carrying system with a total length of 216 m. The bridge which has the span of arch rib is 186m and box-type section has the height and width of the section 2.4 m and 12 m, respectively. 12 vertical columns transmit loads from the deck to the arch ribs. The deck is 12 m wide and



Fig. 2 Some views of the bridge

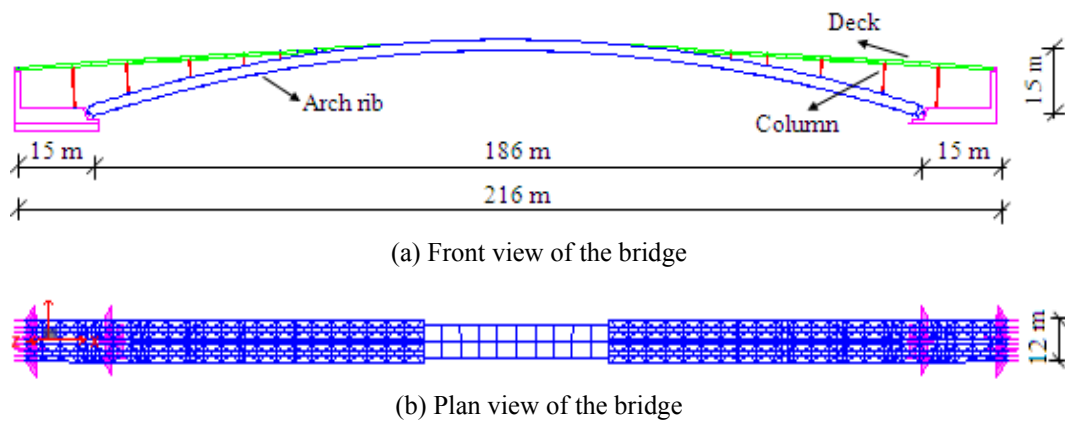


Fig. 3 General arrangements drawing of the bridge

10 cm constant thickness. Along its whole length, the arch ribs and deck are stiffened by horizontal brace members. General arrangement drawings of the entire bridge are shown in Fig. 3.

4. Finite element modelling

Finite element model of the bridge is constituted by SAP2000 software. This software can be used for linear and non-linear, static and dynamic analyses of three dimensional models of engineering structures. In the finite element model, the curve, which defines the axis of the arch, is designed in conformity with the form referred to as the chain curve. Therefore, the occurrence of

moment is restricted under the dead load. Moreover, it is aimed that the arch structural system carries the axial forces. The function expressing the carrier system is given in Eq. (5).

$$y = a \cosh\left(\frac{x}{a}\right) = \frac{a}{2} \left(e^{\frac{x}{a}} + e^{-\frac{x}{a}} \right) \tag{5}$$

where x and y are distance in horizontal and vertical directions and a is a coefficient.

The highway bridge is modelled as a space frame structure with 3D prismatic beam elements which have two end nodes and each end node has six degrees of freedom: three translations along the global axes and three rotations about its axes. The key modelling assumptions are as follows:

- In the finite element model of the bridge, the fictitious elements are used to determine the torsional and M22 moment effects which are consist of asymmetrical load cases. While these elements are defined on the axis through the gravity center of uniform and linear loads, also these elements are modelled as massless.
- In the finite element model of the bridge deck, diagonal fictitious elements are used to reflect the rigid diaphragm effect of the concrete.
- Fictitious elements are modelled as two ends hinged and one end axial sliding.
- Rigid link elements that have great bending rigidity are modelled as two ends rigid to ensure the torsional moments in the carrier system elements.
- In order to determine the length of the rigid element, it is aimed that fictitious elements are located near the gravity center of the loads. The calculation of the gravity center line is given in Fig. 4.

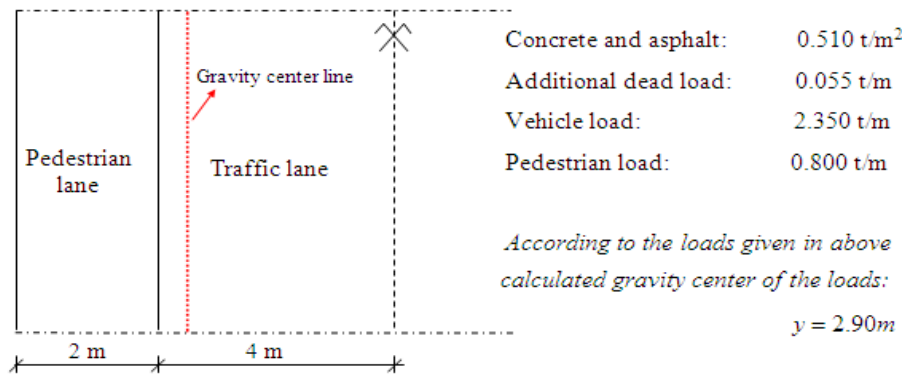


Fig. 4 The calculation of gravity center line location

Table 1 Material properties used in analyses of the highway bridge

Elements	Material Properties		
	Modulus of elasticity (N/m ²)	Poisson's ratio	Mass per unit volume (kg/m ³)
Load bearing elements	2.062E11	0.3	7850
Fictitious elements	2.000E11	0.3	-

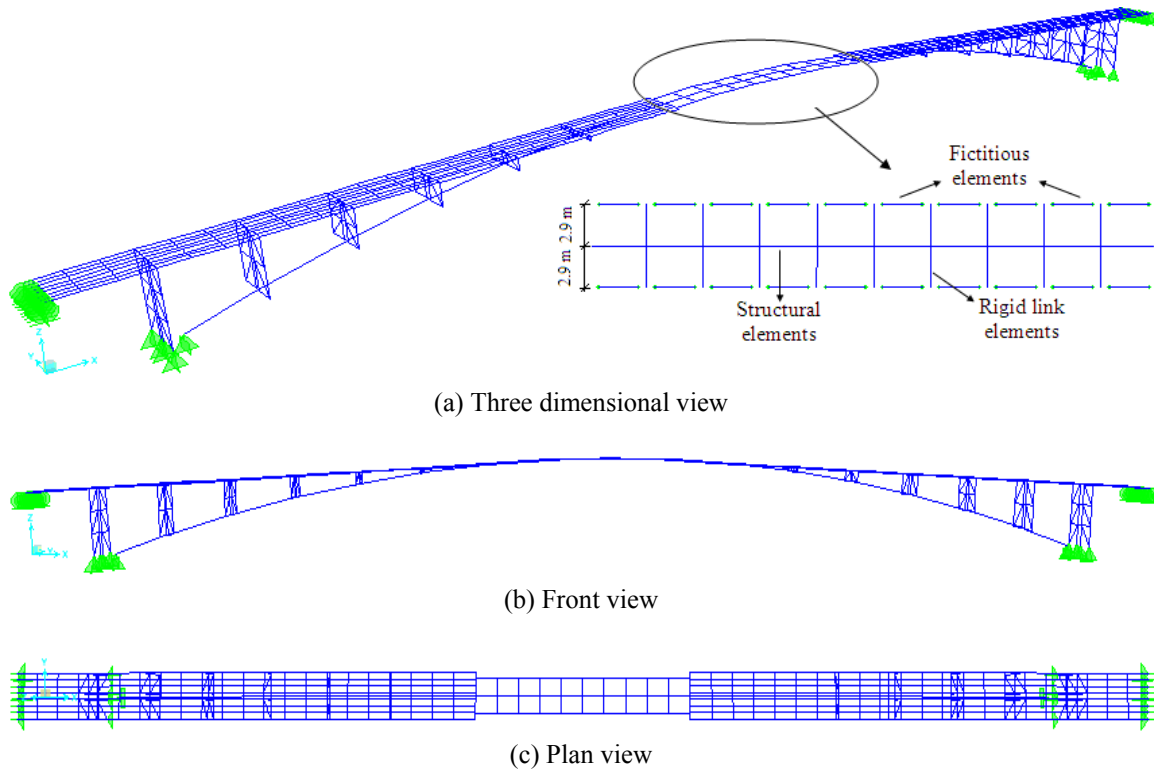


Fig. 5 Three dimensional finite element model of the bridge

For the deck-type arch bridge, the boundary conditions of the side columns connected between the arch and the main girder are fixed to transmit the longitudinal load on the deck. Three dimensional finite element model of Eynel Highway Bridge is given in Fig. 5. The material properties used in analyses is given in Table 1.

Natural frequencies and corresponding mode shapes are the important dynamic characteristics and have significant effect on structural performance of structures. A total of six natural numerical frequencies are obtained which range between 0.614-2.386Hz (Altunışık *et al.* 2011). The first six numerical mode shapes as a whole are shown in Fig. 6.

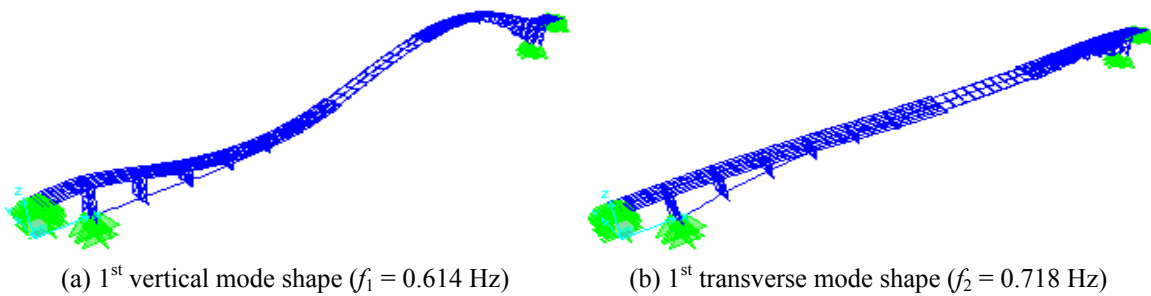


Fig. 6 Numerically identified the first six mode shapes

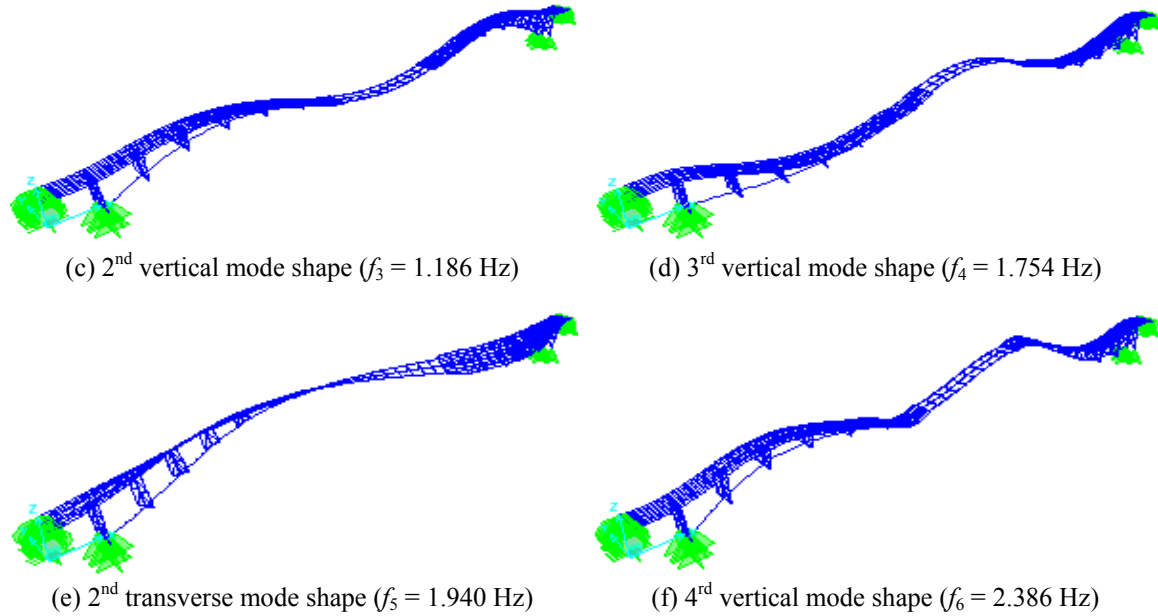
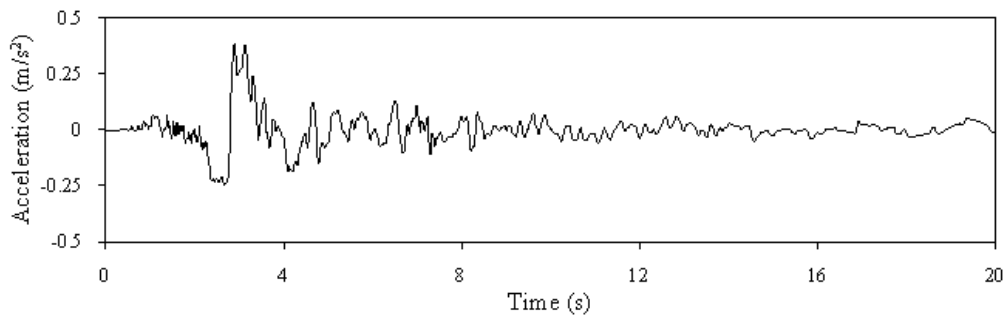


Fig. 6 Continued

5. Seismic performance of bridge

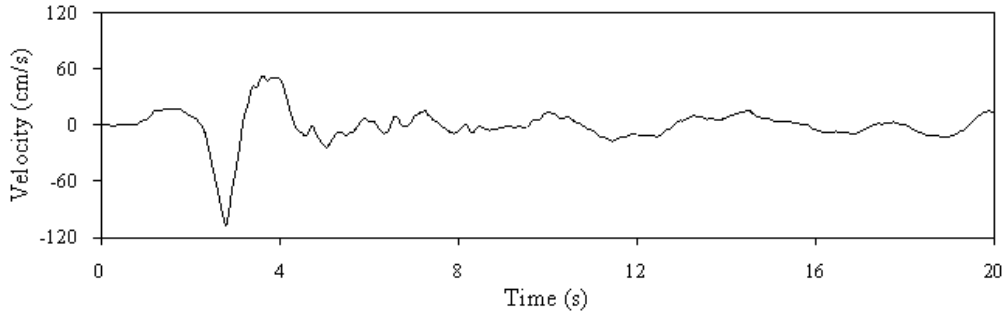
The ERZICAN/ERZ-NS, ERZICAN/ERZ-EW and ERZICAN/ERZ-UP components of 1992 Erzincan earthquake are used as ground motion records. The time-histories of accelerations and velocities of these records with earthquake response spectra considered 5% damping ratio are indicated in Figs. 7-9. The strong ground motion records are obtained from PEER Strong Motion Database (PEER 2016). The databases have information on site conditions and the soil type for instrument locations. Table 2 presents the list the parameters of the ground motion records.

These records are applied to the bridge structure along to the x (longitudinal), y (transverse) and z (vertical) directions simultaneously during analyses. In the first analysis for 0° degree, EW

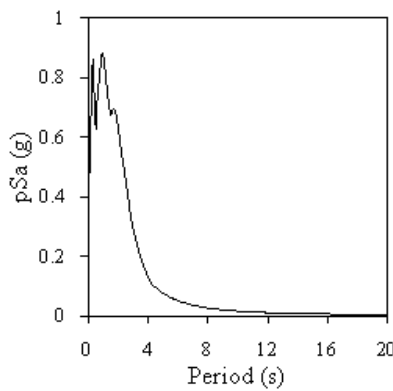


(a) Acceleration time-histories

Fig. 7 The ERZICAN/ERZ-EW component of 1992 Erzincan earthquake



(b) Velocity time-histories

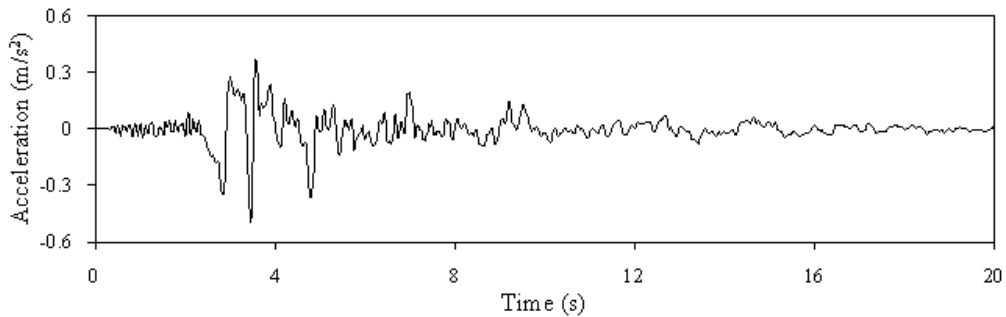


(c) Response spectra with 5% damping ratio

Fig. 7 Continued

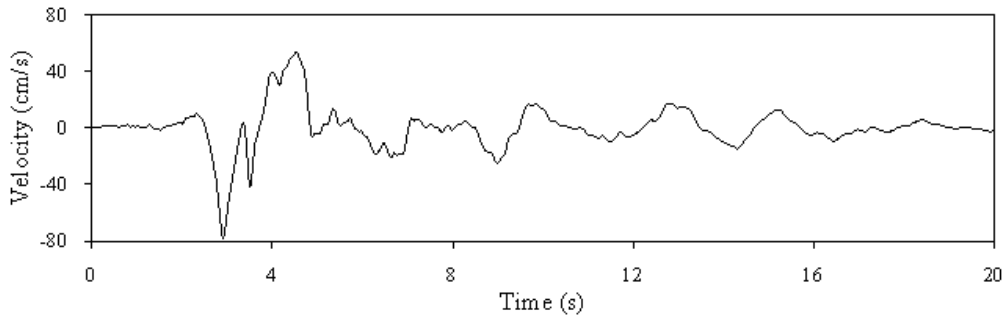
component is applied along to the x direction, NS component is applied along to the y direction and UP component is applied along to the z direction, respectively. Because of the fact that the ground motions and related components are directly important from PEER, scale factor is not considered for vertical component as 0.667.

Ground motions recorded within the near-fault region of an earthquake at stations located toward the direction of the fault rupture are qualitatively quite different from the usual far-fault

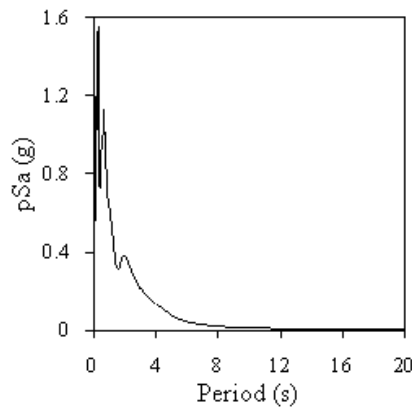


(a) Acceleration time-histories

Fig. 8 The ERZICAN/ERZ-NS component of 1992 Erzincan earthquake



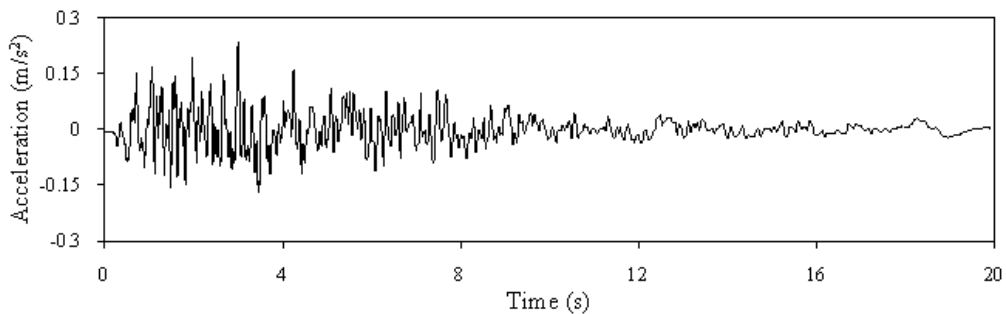
(b) Velocity time-histories



(c) Response spectra with 5% damping ratio

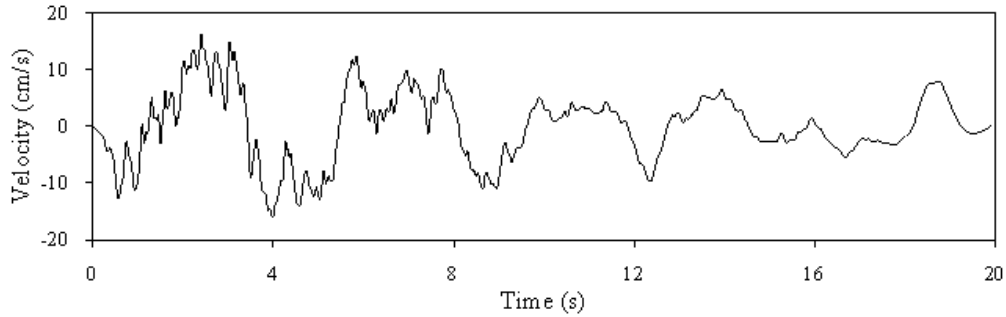
Fig. 8 Continued

earthquake ground motion. Ground motion recorded in the near-fault region displays a long-period pulse in the acceleration history that appears as a coherent pulse in the velocity and displacement histories. Such a pronounced pulse does not exist in ground motions recorded at locations away from the near-fault region (Chopra and Chintanapakdee 2001).

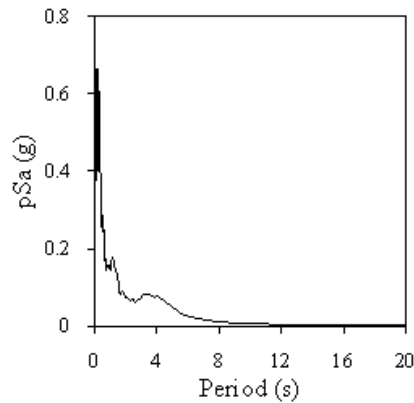


(a) Acceleration time-histories

Fig. 9 The ERZICAN/ERZ-UP component of 1992 Erzincan earthquake



(b) Velocity time-histories



(c) Response spectra with 5% damping ratio

Fig. 9 Continued

Table 2 The detailed information about the strong motion records

No	Near-Fault Strong Ground Motions					
	Earthquake	Component	M	D. km	Site	Peak Ground Acc.
1	1992 Erzincan	NS				0.4961g
2	1992 Erzincan	EW	6.7	4.38	C-D	0.3867g
3	1992 Erzincan	UP				0.2345g

5.1. Displacements

The changing of maximum vertical displacements considering nineteen earthquake angle, whose values ranges between 0 to 90 degrees with an increment of 5 degrees to determine the earthquake angle influence, are given in Fig. 10. To better understanding, the arch geometry is plotted on displacements using bold line. It is seen that the maximum and minimum displacements are obtained as 5.48 cm and 2.34 cm in X direction for 0° and 85° angles, 26.35 cm and 12.29 cm in Y direction for 65° and 0° angles, 19.6 cm and 8.68 cm in Z direction for 65° and 0°, respectively (Table 3). The displacements changed considerably with earthquake angle. The maximum differences are calculated as 57.06%, 114.4% and 55.71% for longitudinal, transverse

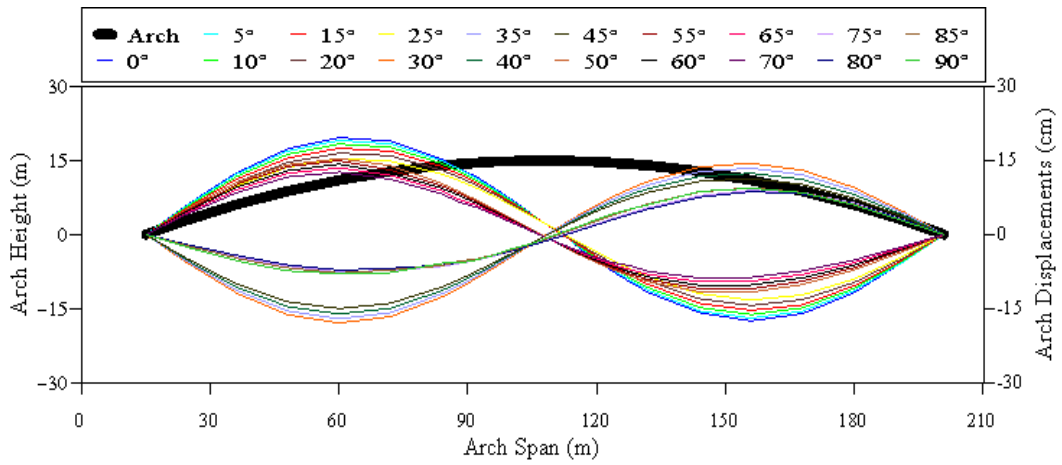


Fig. 10 The changing of maximum vertical displacements along to the bridge arch

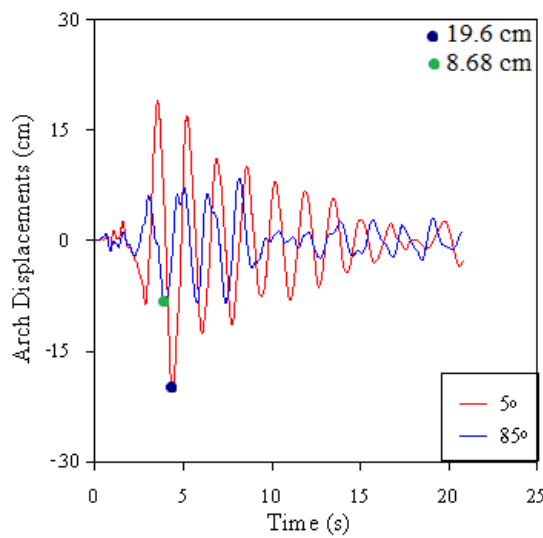


Fig. 11 The time histories of maximum and minimum vertical displacements

Table 3 The maximum differences in displacements for each earthquake angle

Earthquake angle	X direction		Y direction		Z direction	
	Max. displacements (cm)	Diff. (%)	Max. displacements (cm)	Diff. (%)	Max. displacements (cm)	Diff. (%)
0°	5.45	2.75	12.29	12.69	17.32	13.16
5°	5.30	1.89	13.85	11.41	19.60	2.86
10°	5.20	2.69	15.43	11.47	19.04	3.83
15°	5.06	3.56	17.20	9.59	18.31	4.70
20°	4.88	4.10	18.85	8.06	17.45	5.67

Table 3 Continued

Earthquake angle	X direction		Y direction		Z direction	
	Max. displacements (cm)	Diff. (%)	Max. displacements (cm)	Diff. (%)	Max. displacements (cm)	Diff. (%)
25°	4.68	1.28	20.37	6.68	16.46	6.68
30°	4.62	5.19	21.73	2.58	15.36	16.67
35°	4.38	3.42	22.29	7.54	17.92	4.85
40°	4.23	3.31	23.97	3.59	17.05	5.69
45°	4.09	4.16	24.83	2.70	16.08	6.78
50°	3.92	4.59	25.50	1.84	14.99	2.33
55°	3.74	3.21	25.97	1.12	15.34	2.54
60°	3.62	8.29	26.26	0.34	14.95	4.68
65°	3.32	6.93	26.35	0.46	14.25	5.40
70°	3.09	7.77	26.23	1.14	13.48	6.23
75°	2.85	3.51	25.93	1.93	12.64	29.27
80°	2.75	14.91	25.43	2.71	8.94	2.91
85°	2.34	8.97	24.74	3.52	8.68	8.76
90°	2.55	-----	23.87	-----	9.44	-----
	Max. Diff. (%)	57.06	Max. Diff. (%)	114,4	Max. Diff. (%)	55.71

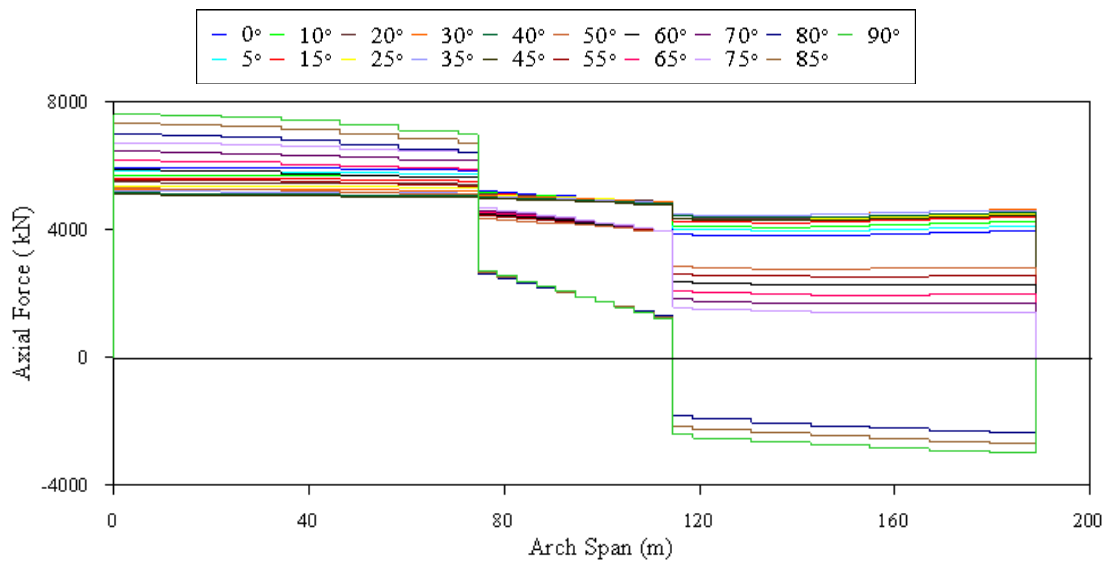


Fig. 12 The changing of maximum axial forces along to the arch length

and vertical directions.

Table 3 presents the maximum differences in each angle and total differences values to evaluate the earthquake angle influence more clearly. The time histories of maximum and minimum vertical

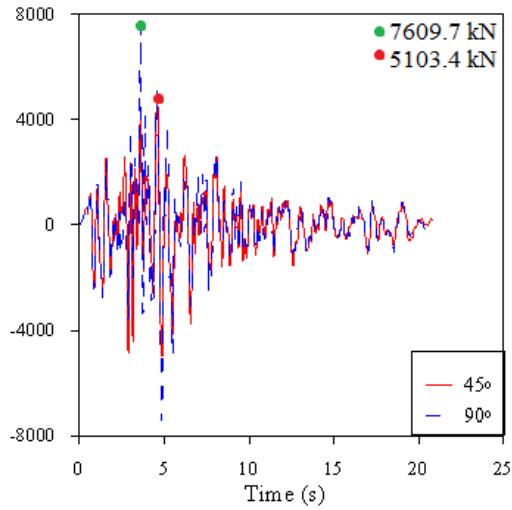


Fig. 13 The time histories of maximum and minimum axial forces

displacements on bridge arch obtained from the linear time-history analysis are given in Fig. 12.

5.2 Internal forces

5.2.1 Bridge arch

To determine the earthquake angle effect on internal forces, the changing of axial forces along to the bridge length for each angle is presented in Fig. 12. It is seen that the axial forces reached the maximum and minimum values at 90° and 45° as 7609.7 kN and 5103.04 kN, respectively (Fig. 12). The axial forces are changed significantly and the maximum differences are calculated as 49.12%.

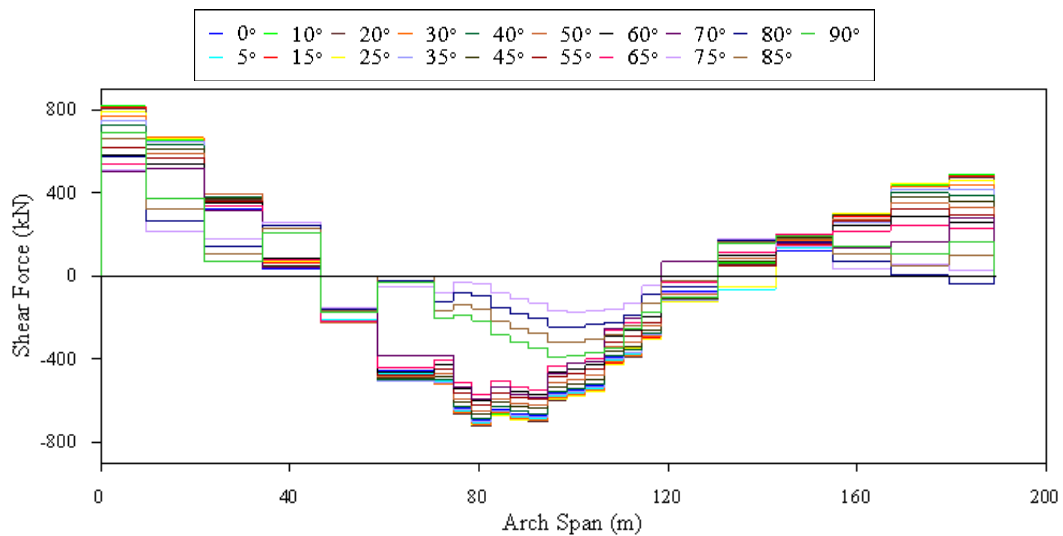


Fig. 14 The changing of maximum shear forces along to the arch length

The time histories of maximum and minimum axial forces obtained from time-history analysis are given in Fig. 13.

The changing of shear forces along to the bridge arch length is shown in Fig. 14. It is seen that the shear forces reached the maximum and minimum values at 5° and 75° as 816.64 kN and 511.47 kN, respectively (Fig. 14). The shear forces are changed significantly and maximum differences are calculated as 37.37%. The time histories of maximum and minimum shear forces are given in Fig. 15.

The changing of maximum bending moments is presented in Fig. 16. It is seen that the bending moments reached the maximum and minimum values at 0° and 85° as 25037.03 kN and 12142.3

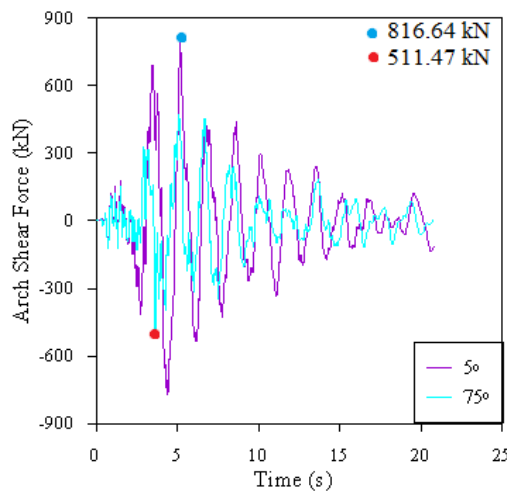


Fig. 15 The time histories of maximum and minimum shear forces

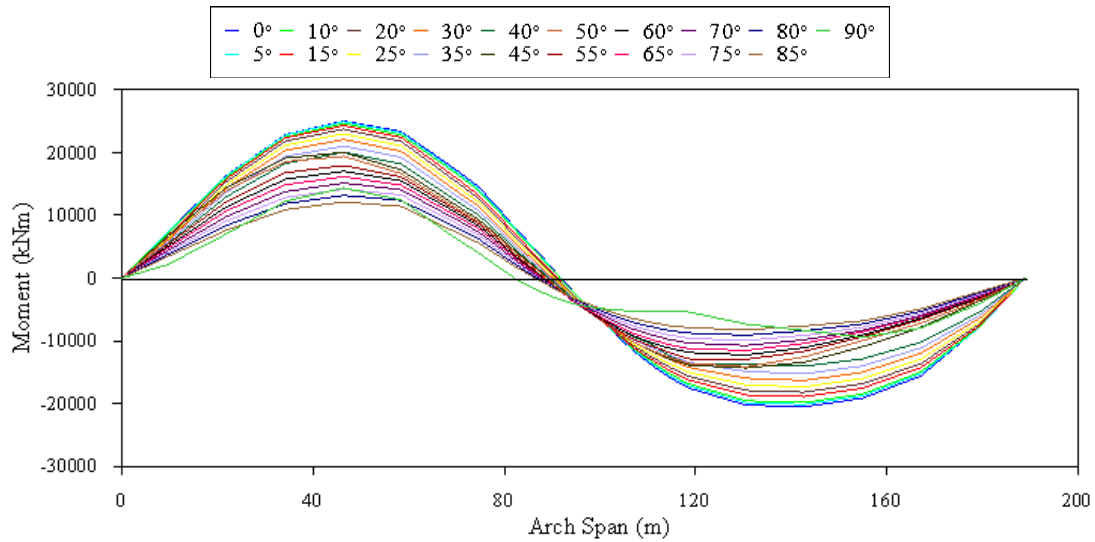


Fig. 16 The changing of maximum bending moments along to the arch length

kN, respectively (Fig. 16). The bending moments are changed significantly and maximum differences are calculated as 51.50%.

The time histories of maximum and minimum bending moments are given in Fig. 17. Table 4 presents the all internal forces, maximum differences in each angle and total differences values to evaluate the earthquake angle influence more clearly.

5.2.2 Bridge deck

The changing of shear forces along to the bridge deck is shown in Fig. 18. It is seen that the shear forces reached the maximum and minimum values at 0° and 70° as 102.48 kN and 51.58 kN, respectively (Fig. 18). The results show that shear forces are changed significantly and maximum differences are calculated as 49.67%.

The time histories of maximum and minimum shear forces obtained from the bridge deck are given in Fig. 19.

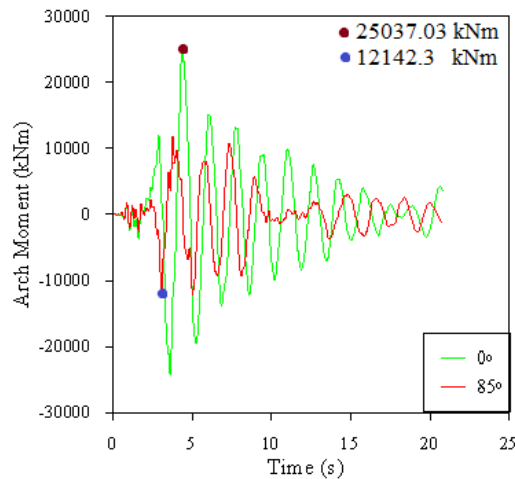


Fig. 17 The time histories of maximum and minimum bending moments

Table 4 The maximum differences in internal forces for bridge deck

Earthquake angle	BRIDGE DECK					
	Max. axial force (kN)	Diff. (%)	Max. shear force (kN)	Diff. (%)	Max. moment (kNm)	Diff. (%)
0°	5952.80	1.91	808.45	1.01	25037.03	0.46
5°	5838.83	2.03	816.64	0.09	24920.80	1.16
10°	5720.39	2.08	815.90	0.45	24632.50	1.39
15°	5601.33	2.03	812.26	1.06	24289.70	2.34
20°	5487.71	1.93	803.69	1.67	23722.01	3.06
25°	5381.72	1.77	790.28	2.28	22996.05	3.93
30°	5286.53	1.50	772.26	2.87	22093.24	4.72
35°	5207.29	1.17	750.13	3.54	21050.25	4.68
40°	5146.24	0.84	723.58	4.26	20064.10	0.15

Table 4 Continued

Earthquake angle	BRIDGE DECK					
	Max. axial force (kN)	Diff. (%)	Max. shear force (kN)	Diff. (%)	Max. moment (kNm)	Diff. (%)
45°	5103.04	3.69	692.79	4.95	20033.65	3.13
50°	5291.22	5.38	658.47	5.74	19407.03	7.57
55°	5575.75	5.20	620.70	6.58	17937.04	5.07
60°	5865.65	4.98	579.88	7.40	17027.91	5.15
65°	6157.70	4.65	536.97	3.91	16150.18	6.19
70°	6443.80	4.24	515.99	0.88	15150.34	6.38
75°	6717.23	4.12	511.47	12.21	14183.41	7.09
80°	6994.20	4.68	573.90	15.68	13177.87	7.86
85°	7321.24	3.94	663.90	4.10	12142.30	18.35
90°	7609.70	-----	691.11	-----	14370.01	-----
	Max. Diff. (%)	49.12	Max. Diff. (%)	37.37	Max. Diff. (%)	51.50

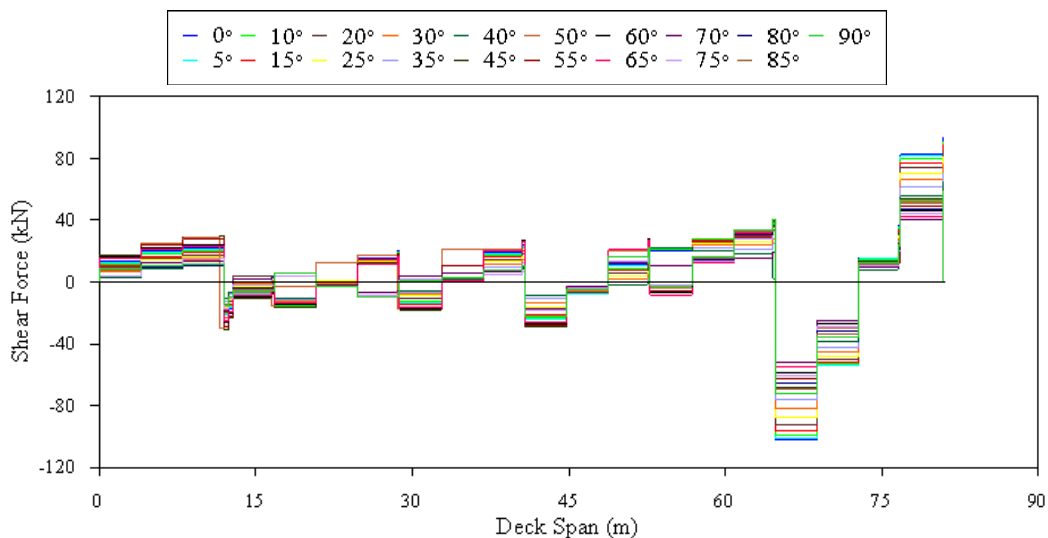


Fig. 18 The changing of maximum shear forces along to the bridge deck

The changing of maximum bending moments for bridge deck is shown in Fig. 20. The bending moments reached the maximum and minimum values at 0° and 70° as 410.69 kN and 208.82 kN, respectively (Fig. 20). The bending moments are changed significantly and maximum differences are calculated as 49.15%.

The time histories of maximum and minimum bending moments obtained from bridge deck for time-history analyses are given in Fig. 21. Table 5 presents the all internal forces, maximum differences in each angle and total differences values to evaluate the earthquake angle influence more clearly.

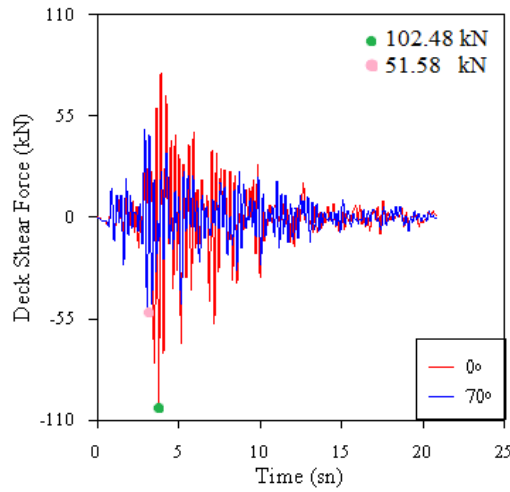


Fig. 19 The time histories of maximum and minimum shear forces for bridge deck

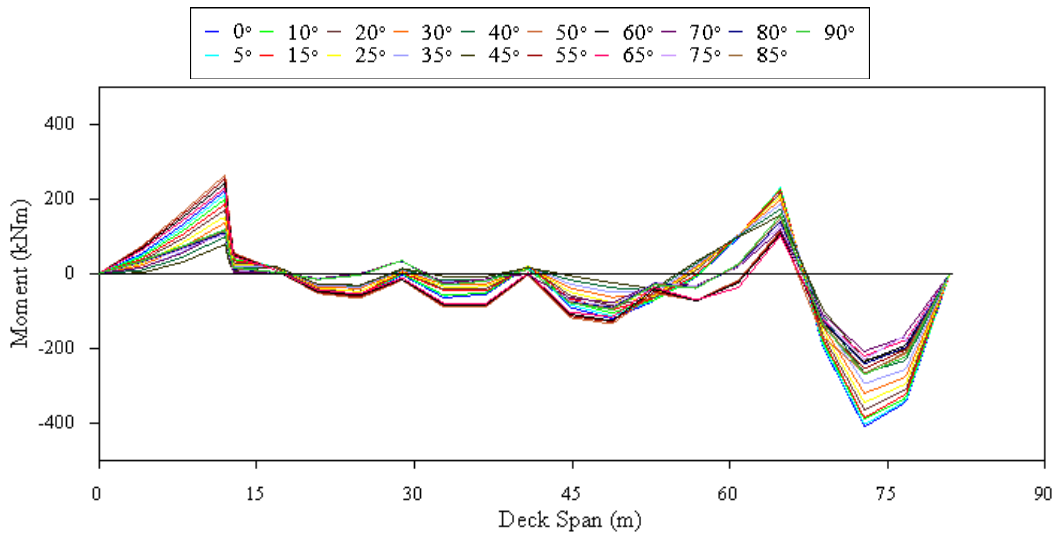


Fig. 20 The changing of maximum bending moments along to the bridge deck

Table 5 The maximum differences in internal forces for bridge deck

Earthquake angle	Bridge deck			
	Max. shear force (kN)	Diff. (%)	Max. moment (kNm)	Diff. (%)
0°	102.48	1.04	410.69	1.47
5°	101.41	1.99	404.64	3.40
10°	99.39	2.97	390.90	0.98
15°	96.44	3.99	387.06	5.54
20°	92.59	5.11	365.60	5.39
25°	87.86	6.35	345.90	7.06

Table 5 Continued

Earthquake angle	Bridge deck			
	Max. shear force (kN)	Diff. (%)	Max. moment (kNm)	Diff. (%)
30°	82.28	7.75	321.47	8.08
35°	75.90	9.39	295.50	9.71
40°	68.77	0.81	266.80	12.93
45°	68.21	3.68	232.30	15.25
50°	65.70	4.57	267.72	4.28
55°	62.70	6.00	256.27	5.33
60°	58.94	6.46	242.60	5.48
65°	55.13	6.44	229.30	8.93
70°	51.58	17.33	208.82	9.96
75°	60.52	7.75	229.62	5.55
80°	65.21	5.98	242.36	10.41
85°	69.11	5.02	267.60	1.26
90°	72.58	-----	270.96	-----
	Max. Diff. (%)	49.67	Max. Diff. (%)	49.15

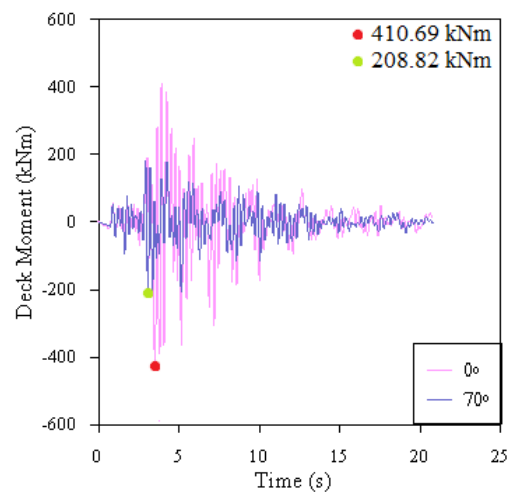


Fig. 21 The time histories of maximum and minimum bending moments for bridge deck

6. Conclusions

This paper presents an investigation about the earthquake angle influence on the seismic performance of arch type steel highway bridges. The bridge is upper-deck steel highway bridge which has arch type carriage system with a total length of 216 m has been analyzed using finite element methods. The bridge is subjected to 1992 Erzincan earthquake ground motion component in nineteen directions whose values ranges between 0 to 90 degrees, with an increment of 5 degrees. The following conclusions are drawn from the study;

- A total of six natural frequencies are obtained which range between 0.614-2.386 Hz. The first six numerical mode shapes are attained as vertical and transverse modes.
- The maximum and minimum horizontal displacements are attained as 5.48 cm and 2.34 cm for 0° and 85° in *X* direction, 26.35 cm and 12.29 cm for 65° and 0° in *Y* direction, 19.6 cm and 8.68 cm for 65° and 0° in *Z* direction, respectively.
- The maximum displacements changed considerably with earthquake angle. These differences are calculated as 57.06%, 114.4% and 55.71% for longitudinal, transverse and vertical directions, respectively.
- The axial forces for bridge arch reached the maximum and minimum values at 90° and 45° as 7609.7 kN and 5103.04 kN. The axial forces are changed significantly and maximum differences are calculated as 49.12%.
- The shear forces for bridge arch reached the maximum and minimum values at 5° and 75° as 816.64 kN and 511.47 kN. The shear forces are changed significantly and maximum differences are calculated as 37.37%.
- The bending moments for bridge arch reached the maximum and minimum values at 0° and 85° as 25037.03 kN and 12142.3 kN. The bending moments are changed significantly and maximum differences are calculated as 51.50%.
- The shear forces for bridge deck reached the maximum and minimum values at 0° and 70° as 102.48 kN and 51.58 kN. The shear forces are changed significantly and maximum differences are calculated as 49.67%.
- The bending moments for bridge deck reached the maximum and minimum values at 0° and 70° as 410.69 kN and 208.82 kN. The bending moments are changed significantly and maximum differences are calculated as 49.15%.

It is shown that structural performance such as dynamic characteristics, displacements and internal forces of the bridge has significantly changed with earthquake ground motion incidence angles. These changes can be seen more clearly for displacement and internal forces. There is not any unique specific angle to attain the maximum or minimum values for each structure. So, structural design of these types of structures should be performed by expert engineers using linear and non-linear finite element analyses considering different earthquake angles to evaluate/consider the more effective combination and to prevent the some dramatical events after earthquakes.

References

- Altunışık, A.C., Bayraktar, A., Sevim, B. and Özdemir, H. (2011), "Experimental and analytical system identification of Eynel arch type steel highway bridge", *J. Construct. Steel Res.*, **67**(12), 1912-1921.
- Athanatopoulou, A.M. (2004), "Critical orientation of three correlated seismic", *Eng. Struct.*, **27**(2), 301-312.
- Armouti, N.S. (2002), "Transverse earthquake-induced forces in continuous bridges", *Struct. Eng. Mech., Int. J.*, **14**(6), 733-738.
- Atak, B., Avşar, Ö. and Yakut, A. (2014), "Directional effect of the strong ground motion on the seismic behavior of skewed bridges", *Proceedings of the 9th International Conference on Structural Dynamics*, Porto, Portugal, June-July.
- Ateş, S., Soyuluk, K., Dumanoğlu, A.A. and Bayraktar, A. (2009), "Earthquake response of isolated cable-stayed bridges under spatially varying ground motions", *Struct. Eng. Mech., Int. J.*, **31**(6), 639-662.
- Bortoli, M.D., Zareian, F. and Shantz, T. (2014), "Significance of ground motion incidence angle in seismic design of bridges", *Proceedings of National Conference on Earthquake Engineering, Frontiers of Earthquake Engineering*, Anchorage, Alaska.

- Chopra, A.K. and Chintanapakdee, C. (2001), "Comparing response of SDF systems to near-fault and far-fault earthquake motions in the context of spectral regions", *Earthq. Eng. Struct. Dyn.*, **30**(12), 1769-1789.
- Cronin, K.J. (2007), "Response sensitivity of highway bridges to random multi-component earthquake excitation", Master Thesis; University of Central Florida, Orlando, FL, USA.
- Eurocode (2004), "EN 1998-1-Eurocode 8: Design of Structures for Earthquake Resistance-Part 1: General Rules, Seismic Actions and Rules for Buildings. [Authority: The European Union Per Regulation 305/2011. Directive 98/34/EC. Directive 2004/18/EC]"
- FEMA, Building Seismic Safety Council for the Federal Emergency Management Agency (2000), FEMA368-NEHRP Recommended Provisions for Seismic Regulations for New Buildings and Other Structures; *Building Seismic Safety Council*, Washington, D.C., USA.
- Fukumoto, Y. and Takewaki, I. (2015), "Critical earthquake input energy to connected building structures using impulse input", *Earthq. Struct.*, **9**(6), 1133-1152.
- Gao, X.A., Zhou, X.Y. and Wang, L. (2004), "Multi-component seismic analysis for irregular structures", *Proceedings of the 13th World Conference on Earthquake Engineering*, Vancouver, B.C., Canada, **1156**, 1-6.
- Gonzalez, P. (1992), "Considering earthquake direction on seismic analysis", *Proceedings of the 10th World Conference on Earthquake Engineering*, Rotterdam, The Netherlands. ISBN: 9054100605
- Kostinakis, K.G. and Athanatopoulou, A.M. (2015), "Evaluation of scalar structure-specific ground motion intensity measures for seismic response prediction of earthquake resistant 3D buildings", *Earthq. Struct.*, **9**(5), 1091-1114.
- Hernandez, J.J. and Lopez, O.A. (2002), "Response to three-component seismic motion of arbitrary direction", *Earthq. Eng. Struct. Dyn.*, **31**(1), 55-77.
- Liang, Z. and Lee, G.C. (2003), "Principal axes of m-dof structures Part II: Dynamic loading", *Earthq. Eng. Eng. Vib.*, **2**(1), 39-50.
- Lopez, O.A. and Torres, R. (1997), "The critical angle of seismic incidence and the maximum structural response", *Earthq. Eng. Struct. Dyn.*, **26**(9), 881-894.
- Mohraz, B. and Tiv, M. (1994), "Orientation of earthquake ground motion in computing response of structures", *Seismic Engineering, Pressure Vessels and Piping Conference*, Minneapolis, MN, USA, pp. 195-202.
- Newton, B. (2014), "Understanding directionality concepts in seismic analysis", *Memo to Designers*, 20-17.
- Ni, Y., Chen, J., Teng, H. and Jiang, H. (2015), "Influence of earthquake input angle on seismic response of curved girder bridge", *J. Traffic Transport. Eng.*, **2**(4), 233-241.
- PEER (2016), Pacific Earthquake Engineering Research Centre. URL: <http://peer.berkeley.edu/smcat/data>
- Prokon (2007), Prokon Engineering and Consultancy Inc., Ankara, Turkey.
- Quadri, S.A. and Madhuri, M.N. (2014), "Investigation of the critical direction of seismic force for the analysis of rcc frames", *Int. J. Civil Eng. Technol.*, **5**(6), 10-15.
- SAP2000 (2015), Integrated Finite Element Analysis and Design of Structures, Computers and Structures Inc., Berkeley, CA, USA.
- Sevim, B. (2013), "Assessment of 3D earthquake response of the Arhavi Highway Tunnel considering soil-structure interaction", *Comput. Concrete, Int. J.*, **11**(1), 51-61.
- Song, B., Pan, J.S. and Liu, Q. (2008), "The study on critical angle to the seismic response of curved bridges based on pushover method", *Proceedings of the 14th World Conference on Earthquake Engineering*, China, October.
- TERDC, Turkish Earthquake Resistant Design Code (2007), Specifications for Structures to be Built in Disaster Areas; Ministry of Public Works and Settlement, General Directorate of Disaster Affairs, Earthquake Research Department, Ankara, Turkey. URL: <http://www.deprem.gov.tr>
- Torbol, M. and Shinozuka, M. (2012), "Effect of the angle of seismic incidence on the fragility curves of bridges", *Earthq. Eng. Struct. Dyn.*, **41**(14), 2111-2124.